



Numerical study on charge transport and electrochemical performance of Gd and Pr co-doped ceria-based solid oxide fuel cells free from internal shorting

Hui Chen¹ · Hui Zhu¹ · Shenglin Shen² · Keqing Zheng² · Yihan Ling^{1,3} · Shaorong Wang³ · Xinxin Wang¹

Received: 28 February 2022 / Revised: 5 April 2022 / Accepted: 7 April 2022 / Published online: 27 April 2022
© The Author(s), under exclusive licence to Springer-Verlag GmbH Germany, part of Springer Nature 2022

Abstract

To guide the composition modification and operation optimization of ceria-based electrolytes of solid oxide fuel cells (SOFCs) for blocking internal electronic current, a one-dimensional model considering the mixed conductivity of oxygen ions and free electrons in Gd and Pr co-doped ceria-based electrolytes $\text{Gd}_{0.1}\text{Pr}_x\text{Ce}_{0.9-x}\text{O}_{1.90}$ (GPDC) was established. The discharge curve, energy efficiency and oxygen partial pressure distribution in ceria-based electrolytes were calculated under different Pr doping contents, operating temperatures and electrolyte thicknesses. The results show that the doping of Pr can relieve internal short circuit current and improve the performance of the cells. The internal short circuit current of the cell increases with raising temperature. With increasing electrolyte thickness, peak power density and leakage current density decrease and the maximum overall efficiency increases. Interestingly, the factor of exponential relationship between electronic conductivity and oxygen partial pressure changes with the doping amount of Pr, and the optimal doping amount of Pr is identified as 0.15 under 700 °C due to the relatively small leakage current density and the high power density. Therefore, this work can guide the design and operation of Gd and Pr co-doped ceria-based electrolyte to develop the highly-efficient low temperature SOFC.

Keywords Solid oxide fuel cells (SOFCs) · Ceria-based electrolyte · Electron-blocking effect · Internal short circuit · Oxygen partial pressure distribution · Gd and Pr co-doped

Introduction

The traditional electrolyte used in solid oxide fuel cells (SOFCs) is ZrO_2 stabilized by Y_2O_3 (YSZ). YSZ needs to be operated at a high temperature of 800 °C ~ 1000 °C [1–4]. CeO_2 doped with three valence rare earth metal such as Gd^{3+} and Sm^{3+} has high oxygen ion conductivity under

the relatively low temperatures due to the abundant oxygen vacancies, which has been widely used to decrease the operating temperature of SOFCs [5, 6]. The ionic conductivity of ceria is about an order of magnitude greater than that of stabilized zirconia under the same doping conditions. Compared with the ion radius of Zr^{4+} , the ion radius of Ce^{4+} is larger, resulting in a more open structure conducive to oxygen ion migration, and therefore ceria-based electrolytes exhibit higher ionic conductivity than zirconia-based electrolyte [7]. However, the reduction of Ce^{4+} to Ce^{3+} of doped CeO_2 can occur under the reducing atmosphere at the anode side of SOFCs, leading to the high electronic conductivity and thus the severe internal short-circuit [8–12].

The design structure of the double-layer electrolyte with an electron-blocking layer has been proposed to reduce the internal electronic current of the cerium-based electrolyte [13, 14]. However, the double-layer electrolyte will increase the ohmic resistance of the cell and the preparation technology is relatively complicated. Therefore, element doping in the ceria-based electrolyte material for reducing its

✉ Xinxin Wang
xxw@cumt.edu.cn

¹ School of Materials Science and Physics, China University of Mining and Technology, Xuzhou 221116, People's Republic of China

² School of Electrical and Power Engineering, China University of Mining and Technology, Xuzhou 221116, People's Republic of China

³ Jiangsu Province Engineering Laboratory of High Efficient Energy Storage Technology and Equipments, China University of Mining and Technology, Xuzhou 221116, People's Republic of China

electronic conductivity might be the promising method to prevent the internal short-circuit. The literature points out [15] doping Pr does not induce bulk lattice changes, but leads to more oxygen vacancies. By doping with Pr, the modified surface property greatly reduced the grain-boundary resistance, leading to an exceptional electrical conductivity. More oxygen vacancies can be introduced into the co-doped structure. The presence of more grain boundaries leads to faster diffusion of oxygen ions [16]. Maricle et al. estimated the electronic conductivity by measuring the total conductivity of $\text{Ce}_{0.8}\text{Gd}_{0.2-x}\text{Pr}_x\text{O}_{1.9}$ at 659–859 °C under low oxygen activity, indicating that the optimal doping of Pr can reduce the conductivity of n-type electrons. However, the literature [17] pointed out that the excessive Pr relative content will cause the increase of electronic conductivity. There is a close relationship between oxygen vacancies and the ratio of $\text{Pr}^{3+}/\text{Pr}^{4+}$ cations. At the low Pr content, Pr^{3+} oxidation state is maintained after calcination. On the contrary, when the doping content x is larger than 0.04, the oxidation of Pr increases. As the content of Pr in the calcined sample increases, the content of Pr^{4+} increases rapidly. Under high oxygen partial pressure, due to the electroosmotic flow effect of $\text{Pr}^{3+}/\text{Pr}^{4+}$ ions in the vicinity of the lattice, the ion mobility number decreases and the electron mobility number increases [18]. Another literature [19] pointed out that Gd-rich, $\text{Ce}_{0.8}\text{Gd}_{0.15}\text{Pr}_{0.15}\text{O}_{1.9}$ has the best conductivity, indicating Pr-doped GDC can obviously enhance the conductivity of the electrolyte. In addition, Pr-doped GDCs not only possess high electrical conductivity, but also can overcome the disadvantage of high electronic conductivity of GDC and SDC under reducing atmosphere. The n-type electronic conductivity of Pr-doped GDC is smaller than GDC under the reducing atmosphere [20].

In this work, building a 1D model to study the electrochemical performance of SOFCs using $\text{Gd}_{0.1}\text{Pr}_x\text{Ce}_{0.9-x}\text{O}_{1.90}$ (GPDC) as electrolyte. Particularly, the factor change of exponential relationship between electronic conductivity and oxygen partial pressure changes with the doping amount of Pr was firstly considered in this numerical study. The influences of temperature, the thickness of electrolyte and different doping concentrations on the performance of single cells were analyzed in terms of open circuit voltage (OCV), internal short circuit current, discharge curve, oxygen partial pressure ($p\text{O}_2$) and efficiencies.

Theoretical model

Since ceria-based electrolyte is a mixed conductivity of electrons and oxygen ions, as shown in Fig. 1, both electrons and oxygen ions can be transferred in the electrolyte. Therefore, part of the electrons reach to the cathode

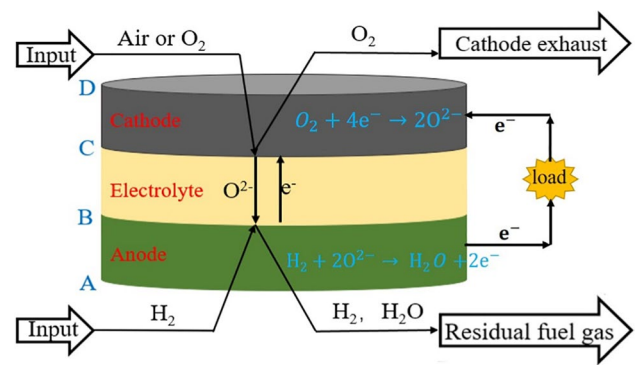
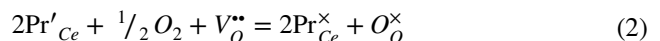
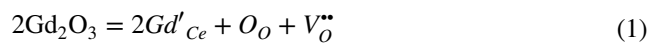


Fig. 1 Schematic diagram of charge transport in SOFC with GPDC electrolyte

through the electrolyte instead of external circuit, causing internal short-circuit and resulting in a decrease of cell performance.

Pr exists in the ceria lattice in two valence states ($\text{Pr}^{3+}, \text{Pr}^{4+}$). The concentration of Pr^{4+} increases with increasing $P(\text{O}_2)$ and decreasing temperature, while the concentration of oxygen vacancies decreases. Under the low oxygen partial pressure, the co-dopants Pr^{3+} and Gd^{3+} generate oxygen vacancies and minimize the interaction between the oxygen vacancies and metal ions, thereby increasing the ionic conductivity and decreasing the electronic conductivity [18, 21].



The chemical expansion increase with the increasing doping content of Pr and the increasing temperature. When Gd and Pr are co-doped, the oxygen vacancies increase with the decreasing oxygen partial pressure, causing the increase of chemical expansion [21]. The thermal expansion coefficient of GPDC is $13.2 \sim 21.5 \times 10^{-6}$ when the doping amount is less than 15% [21]. The thermal expansion coefficients of Ni-YSZ anode and LSCF cathode are, respectively, 13.2×10^{-6} and 13.8×10^{-6} [22]. Therefore, the differences of GPDC electrolyte (the doping amount < 15%) and the electrodes are relatively small ($< 7 \times 10^{-6}$) [23], which would not cause the severe mismatch of thermal expansion coefficients.

The literature [24] shows that when doped with 6% Pr, the peak power density can reach 305 mW cm^{-2} at 750°C . It shows that a small amount of Pr doping has little effect on the single cell structure and performance. Thus, a lower content of Pr doping in the electrolyte is applicable. Besides, the tight connect of electrolyte doped 2% Pr and electrode have been verified by experiments in the related literature [20].

Charge transfer equation in electrolyte

According to the Nernst-Planck, the oxygen ion flux and electron carrier flux in the electrolyte layer can be calculated by the following formulas [25, 26]:

$$\begin{cases} J_{O^{2-}} = -\frac{\sigma_{O^{2-}}}{4F^2} \frac{d\mu_{O^{2-}}}{dx} + \frac{\sigma_{O^{2-}}}{2F} \frac{d\phi}{dx} \\ J_e = -\frac{\sigma_e}{F^2} \frac{d\mu_e}{dx} + \frac{\sigma_{O^{2-}}}{F} \frac{d\phi}{dx} \end{cases} \quad (3)$$

where J is the flux of oxygen ions or charge carriers in the electrolyte layer; μ , σ and ϕ represent the chemical potential, electrical conductivity and electrical potential corresponding to the subscripts.

The operating current density i of SOFC is the sum of the current densities of electrons and oxygen ions, expressed as:

$$i = F(-2J_{O^{2-}} - J_e) \quad (4)$$

For the specific derivation process, please refer to Supplementary Information.

Cell efficiencies

In order to better represent the cell’s leakage and the utilization of cell energy, the voltage, current and the total efficiency of the cell are proposed here. Using the method of Gödickemeier and Gauckler [27, 28] to calculate cell efficiencies. The voltage efficiency ϵ_v can be expressed by the following formula:

$$\epsilon_v = V_{cell}/E \quad (5)$$

The current efficiency ϵ_f can be expressed by:

$$\epsilon_f = i_{ex}/J_{O^{2-}} \quad (6)$$

where i_{ex} is the external electronic.

The total efficiency ϵ is calculated by:

$$\epsilon = \epsilon_v \epsilon_f \quad (7)$$

Table 1 Electronic conductivity and ionic conductivity of GDC electrolyte at different temperatures ($\log P(O_2)=0$) [27]

Temperature/°C	σ_i S/m ⁻¹	σ_e S/m ⁻¹	Exchange current density(A·m ⁻²)	
			Anode	Cathode
600	0.8	5.55×10^{-7}	300	100
650	1.3	3.31×10^{-6}	564	200
700	1.7	9.1×10^{-6}	1000	250
750	2.4	2.735×10^{-5}	1500	350

Modeling and Validation

The mathematical model was built according to the anode support single cell. The model was solved by the simulation software COMSOL MULTIPHYSICS. The conductivity parameters are shown in Table 1. Some parameters can be determined by simultaneously fitting the model results and experimental data. The numerical results are not affected by mesh parameters, which shows the scientific nature of grid division.

Figure 2 shows calculation results and experimental data in the literature [29] I-V and I-P curves of cells. It can be seen that the calculated I-V/I-P curve is in good consistent with the experimental results of the single cell, showing the effectiveness of the model.

In this paper, the leakage current characteristics of several electrolytes are mainly studied, as shown in Table 2.

Discussion

Performance comparison of the single cells using pure GDC and Pr-doped GDC electrolytes

S. Lubke et al. [17] found that the electronic conductivity of pure GDC and doped with low concentration Pr obeyed the

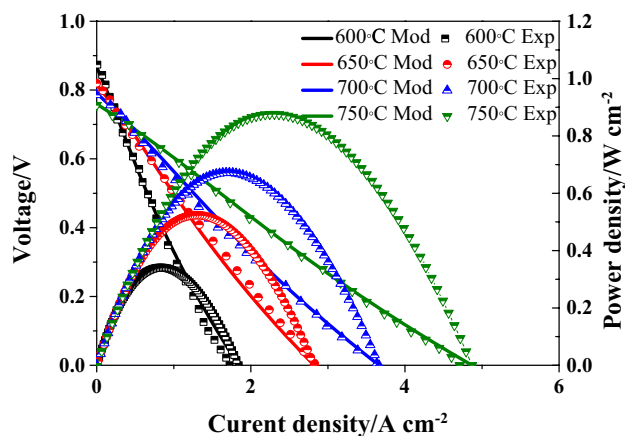


Fig. 2 Calculation results and experimental data I-V/P curves of cells

Table 2 The full name of the abbreviation in the article

Abbreviation	Full name
GPDC5	Gd _{0.1} Pr _{0.05} Ce _{0.85} O _{1.90}
GPDC8	Gd _{0.1} Pr _{0.08} Ce _{0.82} O _{1.90}
GPDC15	Gd _{0.1} Pr _{0.15} Ce _{0.75} O _{1.90}
GPDC25	Gd _{0.1} Pr _{0.25} Ce _{0.65} O _{1.90}
GPDC30	Gd _{0.1} Pr _{0.3} Ce _{0.6} O _{1.90}

-1/5 power of the oxygen partial pressure $P(O_2)$, which is different from the electronic conductivity of GDC following the typical -1/4 [30] power:

$$\sigma_e = \sigma_e^0 P_{O_2}^{-\frac{1}{5}} \quad (8)$$

Figure 3 shows the performance of the cells at different temperatures. With the temperature increases, the internal short circuit current increases, which leads to a decrease in OCV. Compared with pure GDC, the leakage current is much smaller and the open circuit voltage (OCV) is much larger for the GPDC doped with 2 mol% Pr. By comparing Figs. 2 and 3, the peak power density (PPD) using the GPDC electrolyte is much larger than that using pure GDC electrolyte. The higher performance of GPDC can be attributed to that Pr doping will reduce the Gd_2O_3 segregation at the grain boundary to increase the ionic conductivity, and it can also effectively inhibit the reduction of CeO_2 from Ce^{4+} to Ce^{3+} . The electronic conductivity increases with temperature, so the leakage current increases and the OCV of the cell decreases.

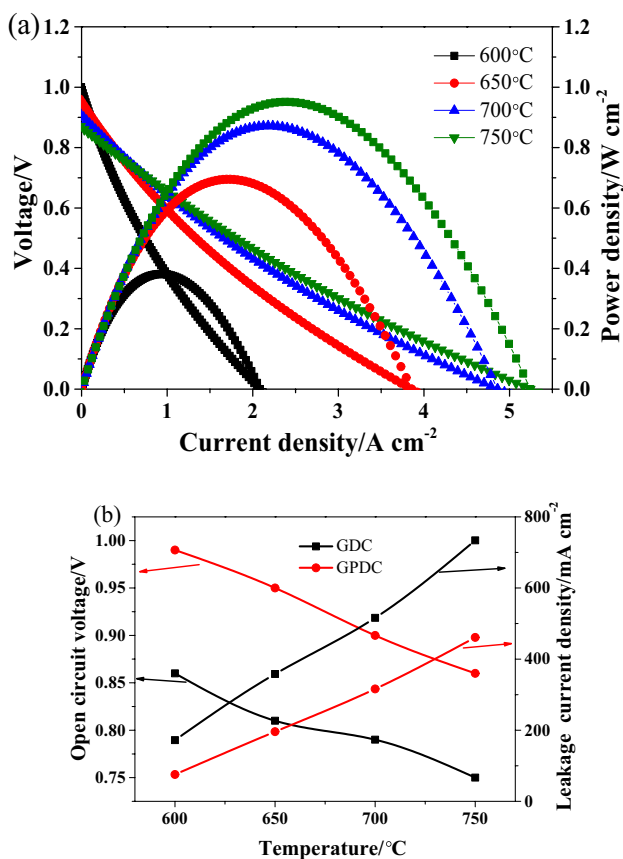


Fig. 3 $Gd_{0.18}Pr_{0.02}Ce_{0.8}O_{1.90}$ as the electrolyte at different temperatures of (a) single cell performance (b) open circuit voltage and leakage current

Figure 4 shows the voltage and total efficiencies of a gadolinium-doped ceria cell under different temperatures. We can also see that the voltage efficiencies decrease linearly as the increase of current density. The change in voltage efficiency is affected by leakage current and polarization loss. It shows that the overall efficiency curve first rises and then drops with current increases. With temperature raises, the short-circuit current increases and the OCV decreases, leading to a decrease in the maximum efficiency. Comparing with the cell using pure GDC, the peak full efficiency of the cell doping with Pr greatly increases from 51.33%, 44.79%, 40.76%, 35.47% to 57.25%, 54.77%, 51.47%, 47.61% under 600°C ~ 750°C. This is because the presence of Pr increases the ionic conductivity and reduces the electronic conductivity.

The performance of $Gd_{0.1}Pr_xCe_{0.9-x}O_{1.90}$ ($x = 0.05, 0.08, 0.15, 0.25, 0.30$) cells with different Pr doping contents

The electronic conductivity of GPDC has a more diverse $P(O_2)$ dependence than that of GDC which follows the typical relationship $\sigma_e = \sigma_e^0 P_{O_2}^{-\frac{1}{4}}$. Lightly doped samples (GPDC5, GPDC8, and GPDC15) have n-type electron conductivity slopes close to -1/4 at low $P(O_2)$, while heavily doped samples (GPDC25, GPDC30) have a reduced slope, especially at low temperatures. Figure 5 shows that a more accurate slope according to the literature [21] is as follows: -1/5 (GPDC5), -1/5 (GPDC8), -3/20 (GPDC15), -3/25 (GPDC25), -1/20 (GPDC30).

The substitution of R for Ce in CeO_2 fluorite structure produces oxygen vacancy by Eq. (9) [31]

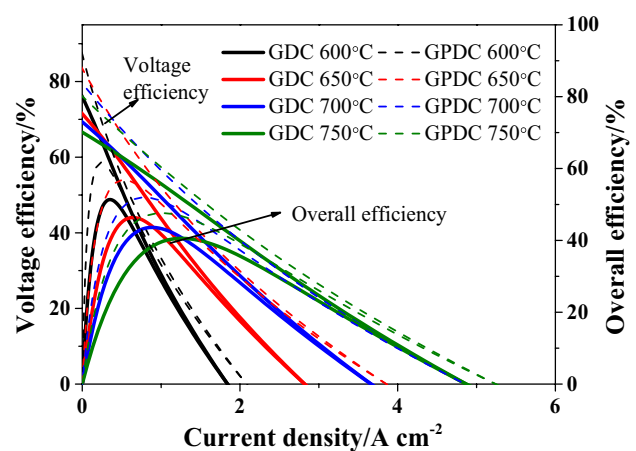


Fig. 4 Voltage efficiency and Overall efficiency of GDC and $Gd_{0.18}Pr_{0.02}Ce_{0.8}O_{1.90}$ as the electrolyte at different temperatures

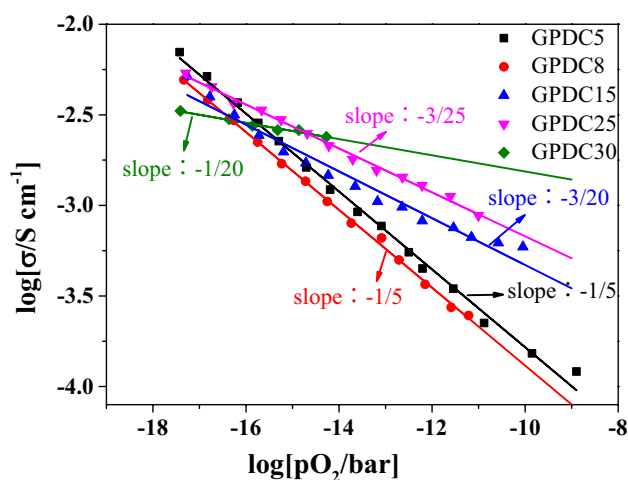
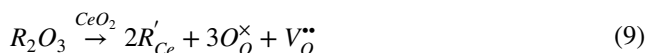


Fig. 5 Logarithm of electronic conductivity of $Gd_{0.1}Pr_xCe_{0.9-x}O_{1.90}$ ($x=0.05,0.08,0.15,0.25,0.30$) versus $\log pO_2$ at $700^\circ C$ [21]



The slope between free electrons and oxygen partial pressure is affected by the following three conditions: (1) The possible interaction between electron and Ce site or O site in RDC; (2) the charge neutrality condition; (3) hopping or no hopping. The doping contents of Pr can influence the choice of above conditions, therefore the slope of relationship curves between electronic conductivity and oxygen partial pressure is different under different Pr doping contents.

It has been demonstrated that the GDC electrolyte doped with Pr has better electrochemical performance. The impact of Pr doping content on the leakage current density is studied according to the electronic and ionic conductivity parameters under different doping contents, which are listed in Table 3 [21]. Theoretically, on the premise that the electrolyte phase structure does not change, the more Pr^{3+} ions with lower valence than Ce^{4+} are doped, the more oxygen vacancies will be generated and the conductivity of oxygen ions will be improved. On the other hand, ion Pr^{3+} with a larger doping radius will make the lattice larger.

Table 3 conductivities (σ_i, σ_e) of GPDC with different Pr doping concentration at $700^\circ C$ ($\log pO_2=0$) [19]

	σ_i S/m ⁻¹	σ_e S/m ⁻¹
GPDC5	2.6	1.5×10^{-5}
GPDC8	2.8	2×10^{-5}
GPDC15	3.2	1.6×10^{-4}
GPDC25	3	3.865×10^{-4}
GPDC30	2	2.20×10^{-3}

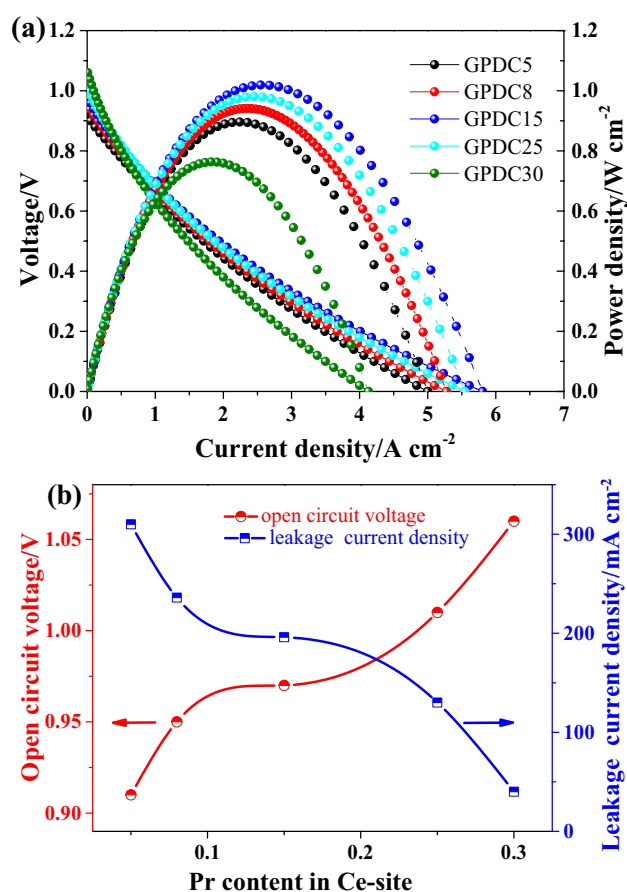


Fig. 6 $Gd_{0.1}Pr_xCe_{0.9-x}O_{1.90}$ ($x=0.05,0.08,0.15,0.25,0.30$) as electrolyte (a) Single cell performance curves (b) OCV and internal short circuit current at $700^\circ C$

A larger lattice constant makes it easier for oxygen ions to pass through, increasing the conductivity of oxygen ions. However, with the further increase of Pr^{3+} doping amount, the increase of lattice oxygen vacancies results in the lattice distortion, causing a decrease of electrical conductivity [20, 24]. So when $x < 0.15$, the ion conductivity increases with the increase of doping amount, but when $x > 0.15$, the ion conductivity decreases with the increasing doping amount. The literature generally indicates maximal ionic conductivity at doping levels between 10 and 20%. The maximum ionic conductivity is a trade-off between the development of deep vacancy associations due to the increased concentration of oxygen vacancies and electrostatic interactions.

The electronic conductivity in ceria-based electrolyte is related to the electron hopping on the ceria sites. Therefore, substitution of Pr for Ce can decrease the ceria site, thus decreasing the electronic conductivity. Besides, the reduction of Pr^{4+} to Pr^{3+} can increase the oxygen vacancy concentration, and the high oxygen vacancy concentration can hinder the electron migration. Pr doping in GDC decreases the electronic conductivity [21].

From Fig. 6(a) we can see that when $0 < x < 0.15$, the electrochemical performance increases with the increase of the Pr doping concentration. When $0.15 < x < 0.30$, as the Pr doping concentration increases, the electrochemical performance decreases. At 700°C , when the doping ratio of Pr is 0.15, the peak power density is 1.02 W cm^{-2} . Figure 6(b) shows that with the increase of Pr doping ratio, the OCV increases, and the internal short circuit current density decreases. Although leakage current is only 40 mA cm^{-2} when doped with 0.3 Pr, the cell power density decreases rapidly, sacrificing the electrochemical performance of the cell. The optimal doping amount should be determined by the tradeoff between reducing leakage current and improving peak power density. From Fig. 6, the optimal doping contents of Pr is 0.15%, and the corresponding leakage current, peak power density and open circuit voltage are, respectively, 195 mA cm^{-2} , 1.02 W cm^{-2} and 0.97 V .

Figure 7 shows that the oxygen partial pressure distribution of different Pr-doped electrolyte cells, when the Pr doping amount is large, $P(\text{O}_2)$ in the electrolyte increases, which resulting in a decrease in the electronic conductivity of the electrolyte and a decrease in Internal short circuit current.

Figure 8 shows the current efficiency increases with the increasing doping. The maximum voltage efficiency under opening also increases with the increasing Pr doping ratio, which can reach 92.98%. Under the high current density, with the increase of Pr doping ratio, the voltage efficiency curve first rises and then drops. The maximum overall efficiency increases with the increasing Pr doping ratio, which can reach 60.22% with the doping concentration of 15%. It can be concluded that the optimal Pr doping concentration is 0.15, which leads to the best electrochemical performance.

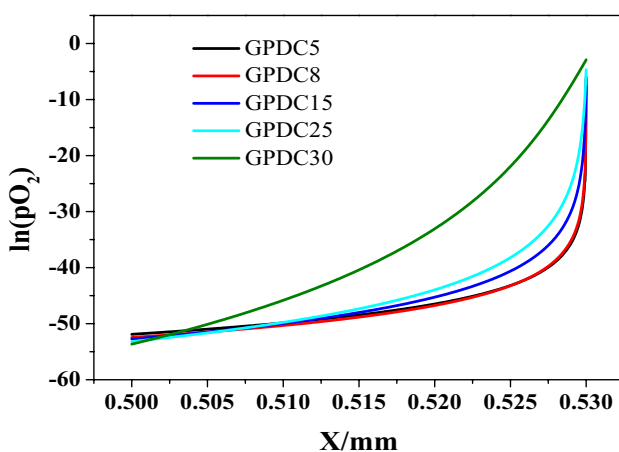


Fig. 7 Oxygen partial pressure distribution of $\text{Gd}_{0.1}\text{Pr}_x\text{Ce}_{0.9-x}\text{O}_{1.90}$ ($x=0.05,0.08,0.15,0.25,0.30$) cells at 700°C

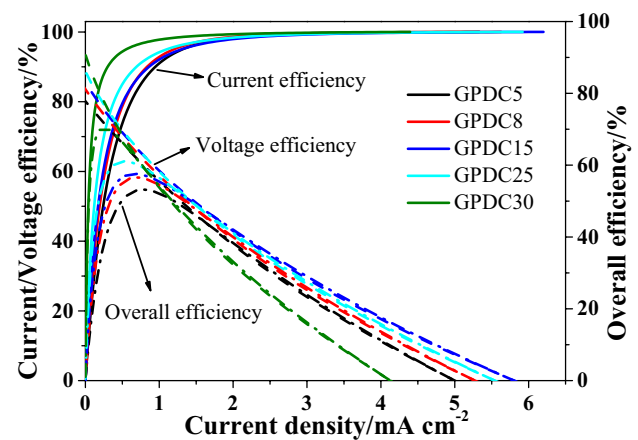


Fig. 8 Current efficiency, Voltage efficiency and Overall efficiency of $\text{Gd}_{0.1}\text{Pr}_x\text{Ce}_{0.9-x}\text{O}_{1.90}$ ($x=0.05,0.08,0.15,0.25,0.30$) cells with different doping at 700°C

The influence of electrolyte thickness on the performance of single cell using GPDC electrolyte

It has been demonstrated the single cell using GPDC electrolyte has much better electrochemical performance. For the sake of further analyzing the effect of the electrolyte thicknesses on the cell performances and leakage, the electrochemical performances of the single cell were calculated by changing the GPDC electrolyte thicknesses for comparison.

At 700°C , the I-V/I-P curves of $\text{Gd}_{0.18}\text{Pr}_{0.02}\text{Ce}_{0.8}\text{O}_{1.90}$ cells with different thicknesses of electrolyte are shown in Fig. 9a. The electrolyte thicknesses are set to $25 \mu\text{m}$, $30 \mu\text{m}$, $40 \mu\text{m}$, $50 \mu\text{m}$, and the corresponding maximum peak power is 0.92 W cm^{-2} , 0.87 W cm^{-2} , 0.79 W cm^{-2} , 0.73 W cm^{-2} . Figure 9b shows as the thickness increases, so does the OCV, and internal short circuit current density drops from 368.2 mA cm^{-2} to 213.9 mA cm^{-2} . When the electrolyte thickness is $50 \mu\text{m}$, the OCV is 0.94 V and the leakage current is 213.9 mA cm^{-2} . This is because the thickness of the electrolyte increases, the ohmic impedance of the cell increases, and the polarization resistance of the cell also increases [32]. Therefore, the appropriate electrolyte thickness should be reasonably selected according to the actual situation.

Figure 10 shows that under the same current density, the current efficiencies rise as the electrolyte thicknesses increases. Under the low discharge current, the voltage efficiencies and the overall efficiencies both increase with the increase of the electrolyte thickness. However, the change rule with electrolyte thickness is opposite under the high discharge current since the increase of electrolyte thickness improves the ohm resistance.

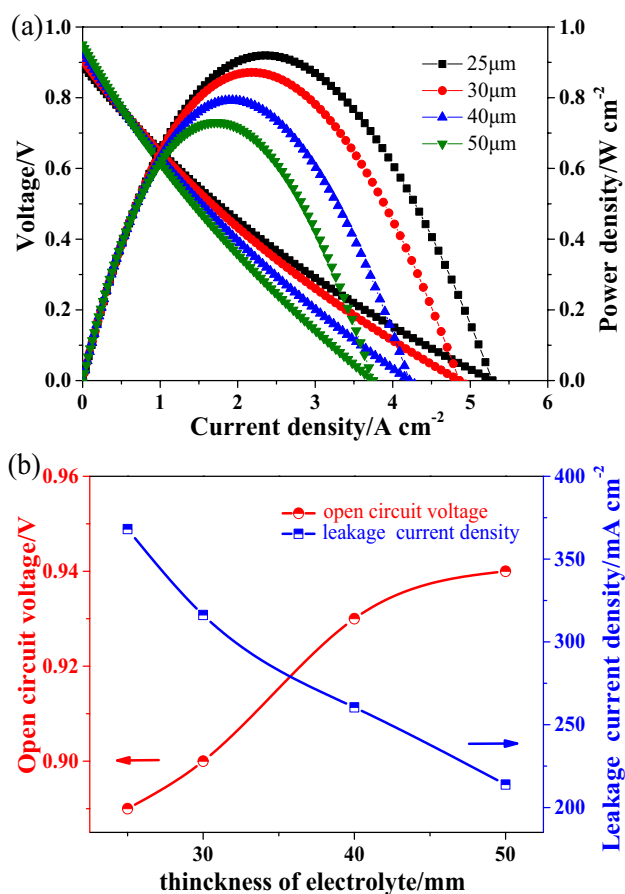


Fig. 9 a I-V/I-P curves (b) OCV and Internal short circuit current density of $Gd_{0.18}Pr_{0.02}Ce_{0.8}O_{1.90}$ cells with different electrolyte thicknesses at 700°C

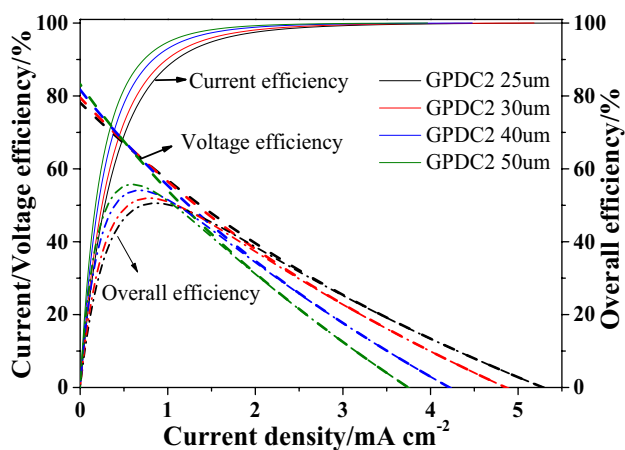


Fig. 10 Current efficiency, Voltage efficiency and overall efficiency of $Gd_{0.18}Pr_{0.02}Ce_{0.8}O_{1.90}$ cells with different electrolyte thicknesses at 700°C

Conclusion

In this work, by reasonably considering the charge transport of electrons and ions, a model was established to analyze the electrochemical performance of cells using GPDC with different doping concentrations as the electrolyte. We can draw the conclusions that:

- (1) It has been demonstrated that the single cell using GPDC has much low leakage current and much higher OCV, PPD and cell efficiency, since the Pr doping in GDC can increase the ionic conductivity and decrease the electronic conductivity.
- (2) The increase of operation temperature can lead to the increase of leakage current and the decrease of OCV and cell overall efficiency. However, oxygen ion conductivity increase with the increasing temperature, thus the peak power density increases.
- (3) The maximum power density and internal short circuit current density of the cells decrease with the increase of electrolyte thickness; the OCV increases with the increasing thicknesses, leading to the rise of maximum overall efficiency. However, due to the increase of ohm resistance, too thick electrolyte will result in a decrease of power density.
- (4) The exponential factor of the exponential relationship between electronic conductivity of GPDC and the oxygen partial pressure increases from $-1/4$ to $-1/20$, which cause that the electronic conductivity decreases with the increasing Pr doping concentration. When the temperature is 700°C and the electrolyte thickness is 50 μm, the optimal doping amount of Pr is 0.15. In this case, the OCV and PPD can reach 0.97 V and 1.02 W cm⁻², and the leakage current density is only 195 mA cm⁻².

Supplementary Information The online version contains supplementary material available at <https://doi.org/10.1007/s11581-022-04563-x>.

Acknowledgements This work was supported by the National Natural Science Foundation of China (No.52104229), the Fundamental Research Funds for the Central Universities (No. 2021QN1105), the Foundation and the Major research project of Jiangsu Key Laboratory of Coal-based Greenhouse Gas Control and Utilization (2020ZDZZ02C)

Data availability All data are available in the manuscript.

Declarations

Conflict of interest The authors declare no competing interests.

References

- Sun MT, Sun JC, Jun JS (2006) Research progress of CeO₂-based solid electrolyte materials. *Chin Rare Earths* 27:78–82. <https://doi.org/10.3969/j.issn.1004-0277.2006.04.019>
- Lin G, Wang X, Rezagadeh A (2021) Electrical energy storage from a combined energy process based on solid oxide fuel cell and use of waste heat. *Sustain Energy Technol Assess* 48:101663. <https://doi.org/10.1016/j.seta.2021.101663>
- Li PZ, Yang W, Tian CJ, Zhao WY, Lu Z, Xie ZP, Wang CA (2021) Electrochemical performance of La₂NiO_{4+δ}-Ce_{0.55}La_{0.45}O_{2-δ} as a promising bifunctional oxygen electrode for reversible solid oxide cells. *J. Adv. Ceram.* 10328–337
- Cao D, Zhou MY, Liu ZJ, Yan XM, Liu J (2020) Fabrication and Characterization of Anode-supported Solid Oxide Fuel Cell Based on Proton Conductor Electrolyte. *J Inorg Mater* 35:1047–1052
- Narayanan M, Mengedoht G, Commerell W (2021) Evaluation of SOFC-CHP's ability to integrate thermal and electrical energy system decentrally in a single-family house with model predictive controller. *Sustain Energy Technol Assess* 48:101643. <https://doi.org/10.1016/j.seta.2021.101643>
- Ling YH, Wang XX, Ma ZK, Wei KW, Wu YJ, Khan M, Wang SR (2019) Review of experimental and modelling developments for ceria-based solid oxide fuel cells free from internal short circuits. *J Mater Sci* 55:1–23. <https://doi.org/10.1007/s10853-019-03876-z>
- Jaiswal N, Tanwar K, Suman R, Kumar D, Upadhyay S, Parkash O (2019) A brief review on ceria based solid electrolytes for solid oxide fuel cells. *J Alloys Compd* 781:984–1005. <https://doi.org/10.1016/j.jallcom.2018.12.015>
- Fu Q, Saltsburg H, Flytzani-stephanopoulos M (2003) Active non-metallic Au and Pt species on ceria-based water-gas shift catalysts. *Science* 301:935–938. <https://doi.org/10.1126/science.1085721>
- Xu J, Wang LC, Liu YM, Cao Y, He HY, Fan KN (2009) Meso-structured CeO₂ as an effective catalyst for styrene synthesis by oxidative dehydrogenation of ethylbenzene. *Catal Lett* 133:307–313. <https://doi.org/10.1007/s10562-009-0174-x>
- Zeng S, Zhang W, Guo S, Su H (2012) Inverse rod-like CeO₂ supported on CuO prepared by hydrothermal method for preferential oxidation of carbon monoxide. *Catal Commun* 23:62–66. <https://doi.org/10.1016/j.catcom.2012.02.028>
- Zhou K, Wang X, Sun X, Peng Q, Li Y (2005) Enhanced catalytic activity of ceria nanorods from well-defined reactive crystal planes. *J Catal* 229:206–212. <https://doi.org/10.1016/j.jcat.2004.11.004>
- Jobbágy M, Mariño F, Schönbrod B, Baronetti G, Laborde M (2006) Synthesis of Copper-Promoted CeO₂ Catalysts. *Chem Mater* 18:1945–1950. <https://doi.org/10.1021/cm052437h>
- Ma ZK, Song Z, Wang XX, Ou XM, Zheng K, Guo LM, Feng PZ, Wang SR, Zhou FB, Ling YH (2019) Numerical Study on the Electron-blocking Mechanism of Ceria-related Composite Electrolytes Considering Mixed Conductivities of Free Electron, Oxygen-ion and Proton. *ACS Appl Energy Mater* 2:3142–3150
- Ling YH, Guo TM, Guo YY, Yang Y, Tian YF, Wang XX, Ou XM, Feng PZ (2021) New two-layer Ruddlesden-Popper cathode materials for protonic ceramics fuel cells. *J Adv Ceram* 10:1052–1060
- Liu Y, Fan L, Cai Y, Zhang W, Wang B, Zhu B (2017) Superionic Conductivity of Sm⁽³⁺⁾, Pr⁽³⁺⁾, and Nd⁽³⁺⁾ Triple-Doped Ceria through Bulk and Surface Two-Step Doping Approach. *ACS Appl Mater Interfaces* 9:23614–23623. <https://doi.org/10.1021/acsami.7b02224>
- Arabacı A (2018) Synthesis and characterization of Pr/Gd co-doped ceria by using the citric acid-nitrate combustion method. *Solid State Ion* 326:69–76. <https://doi.org/10.1016/j.ssi.2018.09.012>
- Lubke S, Wiemhofer HD (1999) Electronic conductivity of Gd-doped ceria with additional Pr-doping. *Solid State Ion* 117:229–243. [https://doi.org/10.1016/S0167-2738\(98\)00408-1](https://doi.org/10.1016/S0167-2738(98)00408-1)
- Spiridigliozzi L, Dell'Agli G, Accardo G, Yoon SP, Frattini D (2019) Electro-morphological, structural, thermal and ionic conduction properties of Gd/Pr co-doped ceria electrolytes exhibiting mixed Pr³⁺/Pr⁴⁺ cations. *Ceram Int* 45:4570–4580. <https://doi.org/10.1016/j.ceramint>
- Dholabhai PP, Adams JB, Crozier PA, Sharma R (2011) In search of enhanced electrolyte materials: a case study of doubly doped ceria. *J Mater Chem* 21:18991
- Cheng YC (2013) Pr · Gd co-doped ceria based materials in IT-SOFC. Chemistry College of Science National Taiwan University.
- Cheng SY, Chatzichristodoulou C, Søgaaard M, Kaiser A, Hendriksen PV (2017) Ionic/Electronic Conductivity, Thermal/Chemical Expansion and Oxygen Permeation in Pr and Gd Co-Doped Ceria Pr_xGd_{0.1}Ce_{0.9-x}O_{1.95-δ}. *J Electrochem Soc* 164:1354–1367. <https://doi.org/10.1149/2.0531713jes>
- Yu JF, Luo LH, Cheng L, Xu X, Wang LY, Yu YZ, Xia CK (2022) The Research Progress for Perovskite-structure SOFC Cathode Materials. *Mater Rep* 36:11–21
- Huang ZY (2020) Study on the supporter of nickel-based cermet anodes for intermediate temperature solid oxide fuel cells. Tianjin University.
- Grazia A, Gianfranco DA, Luca S, Sung PY, Domenico F (2020) On the oxygen vacancies optimization through Pr co-doping of ceria-based electrolytes for electrolyte-supported solid oxide fuel cells. *Int J Hydrogen Energy* 38(45):19707–19719. <https://doi.org/10.1016/j.ijhydene.2020.05.011>
- Wang XX, Ma ZK, Zhang T, Kang JH, Ou XM, Feng PZ, Wang SR, Zhou FB, Ling YH (2018) Charge-Transfer modeling and polarization DRT analysis of proton ceramics fuel cells based on mixed conductive electrolyte with the modified anode-electrolyte interface. *ACS Appl Mater Interfaces* 41:35047–35059. <https://doi.org/10.1021/acsami.8b10429>
- Wang XX, Zhang T, Kang JH, Zhao L, Guo LT, Feng PZ, Zhou FB, Ling YH (2017) Numerical modeling of ceria-based SOFCs with bi-layer electrolyte free from internal short circuit: comparison of two cell configurations. *Electrochim Acta* 248:356–367
- Wang XX, Wei KW, Kang JH, Shen SL, Budiman RA, Ou XM, Zhou FB, Ling YH (2018) Experimental and numerical studies of a bifunctional proton conducting anode of ceria-based SOFCs free from internal shorting and carbon deposition. *Electrochim Acta* 264:109–118
- Gödicke-meier M, Gauckler LJ (1998) Engineering of solid oxide fuel cells with ceria-based electrolytes. *J Electrochem Soc* 145:414–421
- Zhen YD, Tok AIY, Jiang SP, Boey FYC (2008) Fabrication and performance of gadolinia-doped ceria-based intermediate-temperature solid oxide fuel cells. *J Power Sources* 178:69–74. <https://doi.org/10.1016/j.jpowsour.2007.11.113>
- Steele BCH (2000) Appraisal of Ce_{1-y}Gd_yO_{2-y/2} electrolytes for IT-SOFC operation at 500°C. *Solid State Ion* 129:95–110
- Taro S, Yoshihiro H, Yuka E, Sa S, Teruhisa H, Harumi Y (2004) Electronic conductivity measurement of Sm and La-doped ceria ceramics by Hebb-Wagner method. *Solid State Ion* 174:27–33. <https://doi.org/10.1016/j.ssi.2004.07.025>
- Park B-K, Barnett SA (2020) Boosting solid oxide fuel cell performance via electrolyte thickness reduction and cathode infiltration. *J Mater Chem A* 8(23):11626–11631. <https://doi.org/10.1039/d0ta04280c>

Publisher's note Springer Nature remains neutral with regard to jurisdictional claims in published maps and institutional affiliations.